CHAPTER 2
BACKGROUND AND THEORIES

2.1 General climate of Thailand

Thailand lies within the tropics and the general climate is mainly influenced by two monsoons (southwest and northeast) (TMD, 2012; Torsri et al., 2013). The southwest monsoon brings about a rainy season for most of the country between mid-May and mid-October, as a result of warm moist air transported from the Indian Ocean. Synoptic winds during this period flow from the south, southwest and west directions in different parts of the country. The northeast monsoon starts around mid-October and lasts till mid-February, bringing cold and dry air from high-pressure areas in mainland China. The weather in the transition period from the northeast monsoon to the southwest monsoon, around from mid-February to mid-May, is generally the warmest, and also influenced by the southerly gulf winds over the Central and Eastern regions.

2.2 Wind resource assessments in Thailand

Increased interest in renewable energy in Thailand has motivated various wind resource assessments. A first study (Exell, 1985) statistically analyzed observed 10-m wind speed data from 1951-1960 and found mean power density of 30-230 W m^{-2} at a station in Chanthaburi, Eastern region. World Bank (2001) produced yearly and seasonal wind maps for Thailand, Cambodia, Laos and Vietnam at 30-m and 65-m above ground level (AGL), and wind power density at 65-m (hereafter, all heights refer to meters AGL). The study had applied 1-km resolution mesoscale modeling. The regional wind maps from the study show mean wind speeds of 5.5-6.0 m s^{-1} and wind power density of 200-320 W m^{-2} for the Eastern region, while for other parts showed some reasonable potential such as in the North-Eastern region.

In 2001, the Department of Energy Development and Promotion (currently, the Department of Alternative Energy Development and Efficiency) published wind maps of 1-km resolution for heights of 10 m, 30 m and 50 m over Thailand. The study found the values of annual mean wind speed to be about 6.4 m s^{-1} at 50 m for the Eastern region

adjacent to the Gulf of Thailand. In 2010, Manomaiphiboon et al. (2010) applied mesoscale (MM5) and microscale (CALMET) modeling over Thailand to generate 1-km resolution wind maps at multiple heights, showing that annual average 100-m wind speed is 4-8 m s^{-1} over the Eastern region (Figure 2.1). Paton and Manomaiphiboon (2013) estimated wind resource potential over Bangkok Province, using 1-km resolution mesoscale modeling with refined land-use and land-cover data from satellite imagery, finding a relatively large potential in southwest Bangkok adjacent to the coast with 200 W m^{-2} and but lower potential for the city with 125 W m^{-2} at heights of 100 m.

2.3 Winds and wind power

Winds in the free atmosphere are caused by the presence of high and low pressure zones resulting from the uneven incident solar radiation on the earth's surface. The flow is further affected by rotation of the earth, and within a boundary layer, turbulence from friction with the earth's surface (Manwell et al., 2002). The boundary layer is the depth of the atmosphere under the influence of surface processes. It varies with time of day, depending on surface mixing. During the day, as the sun heats the earth's surface, heat transfer to the cooler atmosphere results in higher mixing by convection which causes the boundary layer to increase to a height of 1-2 km. At night, the heat transfer reverses as the earth's surface cools faster, subsequently reducing the mixing and boundary layer to a height of 100 m (Oke, 1987). Synoptic winds are associated with scales of atmospheric motion such as weather fronts of magnitude ranging from 500-10,000 km and appear in the form geostrophic winds, gradient winds, and the winds due to rotational motion. The Coriolis force and surface friction cause counterclockwise flow into and around a low pressure area and clockwise around a high pressure area for the northern hemisphere, with a reversal of this pattern in the southern hemisphere (Manwell et al., 2002). Further, there are local effects such as eddies, turbulence and thermals on a smaller scale as shown in Figure 2.2.

Sea and land breezes are the result of factors such as physical features and land-sea temperature contrast (Phan and Manomaiphiboon, 2012). Land-sea breezes arise from the different rates at which land and water masses absorb or release heat due to heating from

the sun. Land heats up and cools down faster than water, which has a higher heat capacity, and at a location where the two meet, during the day the land will absorb heat faster and then at night, it will cool faster. During the day, the land is relatively warmer, heating up the air which rises to be replaced by the cooler air from the sea; this flow is called the sea breeze. At night, the water mass is warmer and the air rises above it to be replaced by cooler air from the land, resulting in the land breeze. Mountain and valley breezes result from uneven heating of mountain slopes by the sun, where during the day the slopes are heated up and the air which has been warmed rises to be replaced by cooler air from the foot of the mountain. This flow is known as the valley breeze. Mountain breeze occurs in the late evening and at night as the mountain peaks cool down faster and the cold air flows down through the valley to the base of the mountain (Gipe, 2004).

2.3.1 Logarithmic profile

The variation of mean wind speed with height u (m s^{-1}), in the surface layer can be expressed as a log-law wind profile,

$$u(z) = \frac{u_*}{\kappa}\left[\ln\left(\frac{z}{z_0}\right) + 6\frac{z}{L}\right], \tag{2.1}$$

where u_* is the friction velocity (m s^{-1}), z is the height above ground level (m), κ is the von Kármán constant (~0.4), z_0 is the roughness length (m) and L is the Monin-Obhukov length (m). L is mathematically expressed by

$$L = \frac{-u_*^{\,3}}{\kappa \cdot (g/T_v) \cdot H}, \tag{2.2}$$

where g is the acceleration due to gravity, T_v is the absolute virtual temperature (K), and H is the kinematic surface heat flux (K·m s^{-1}). L is negative under unstable conditions and

positive for stable conditions. Figure 2.3 shows the wind speed profiles for different atmospheric boundary layer stability conditions. The wind speed profile is reduced in unstable conditions (daytime) and increased during stable conditions such as during the night (Petersen et al., 1998; Stull, 2000)

2.3.2 Power law profile

Under neutral conditions and the lack of roughness classes, the power law model can be used to approximate wind speeds at higher heights:

$$\frac{u_2}{u_1} = \left(\frac{z_2}{z_1}\right)^{\alpha}, \tag{2.3}$$

where u_1 is the wind speed (m s^{-1}) at the reference height z_1 (m), and u_2 is the wind speed at height z_2, and α is the wind shear exponent whose value varies with terrain and atmospheric stability. Under neutral conditions, a typical value of 0.14 is normally assigned for α (Manwell et al., 2002).

2.3.3 Power from Winds

The power obtainable from the wind, P_{wind} (W) is given by,

$$P_{\text{wind}} = \frac{1}{2}\rho_a u^3 A, \tag{2.4}$$

where ρ_a is the density of air (kg m^{-3}), A is the cross-sectional area of a wind turbine (m^2), u is the wind speed (m s^{-1}). The maximum theoretical wind power that can be extracted by a wind turbine is given by the Betz limit at 59%. As can be seen, the elements affecting the power available in the wind stream are the air density, area of the wind turbine rotor and the wind speed. However, the influence of the wind speed is more

prominent owing to its cubic relationship with the power. In the case of wind speed forecasting applications, a model giving a 10% over prediction would lead to the wind power being over-predicted by 33%, whereas a 10% under prediction would lead to a 27% under-prediction of the wind power. Thus, the accurate prediction of wind speed is important for wind energy applications.

(Intentionally left blank)

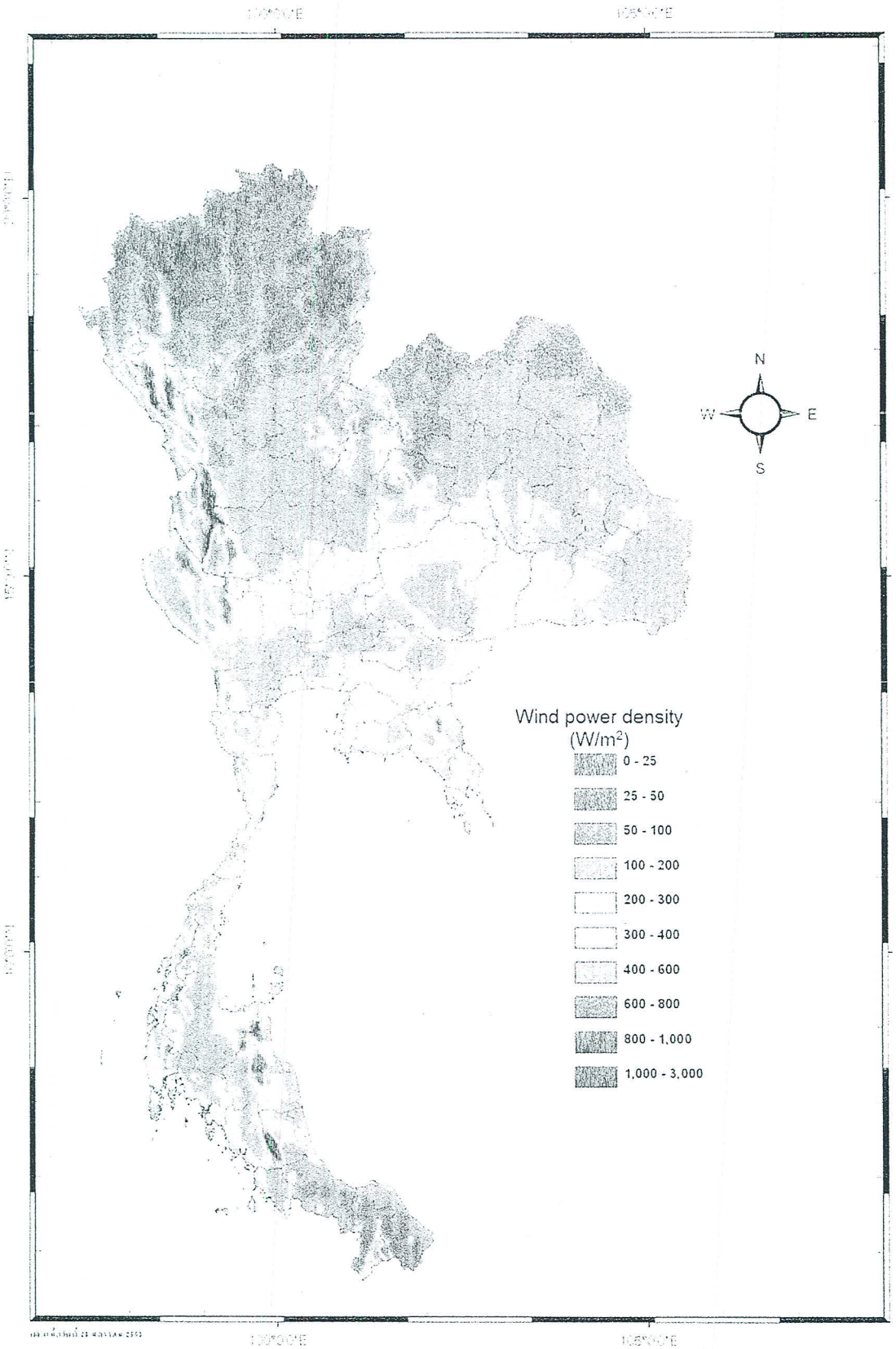

Figure 2.1: Annual 100-m wind power density over Thailand

(Adapted from Manomaiphiboon et al., 2010)

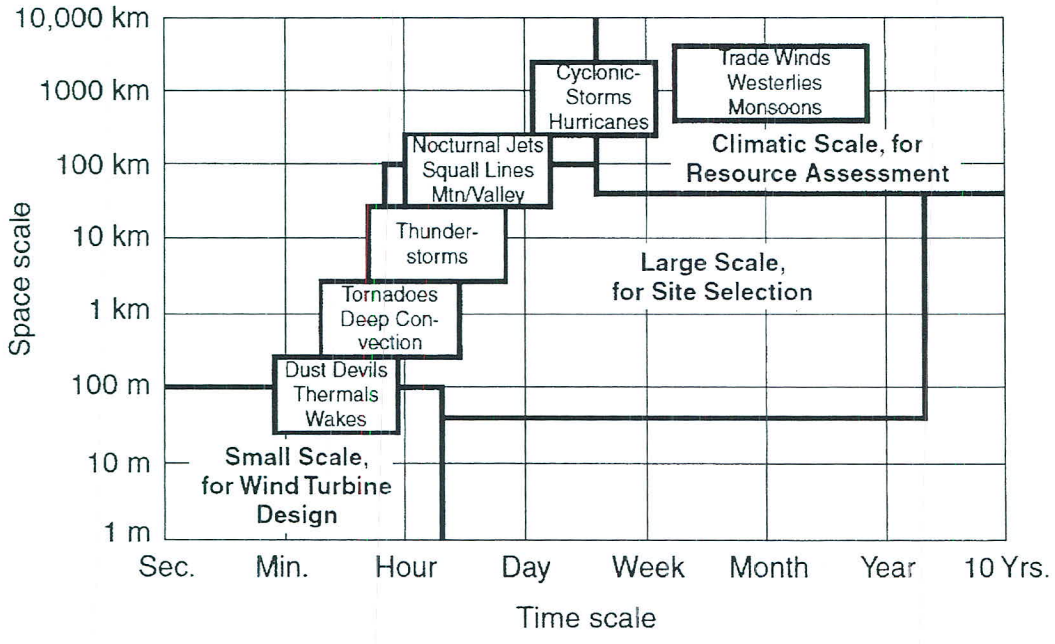

Figure 2.2: Atmospheric scales of motion (Source: Manwell et al., 2002)

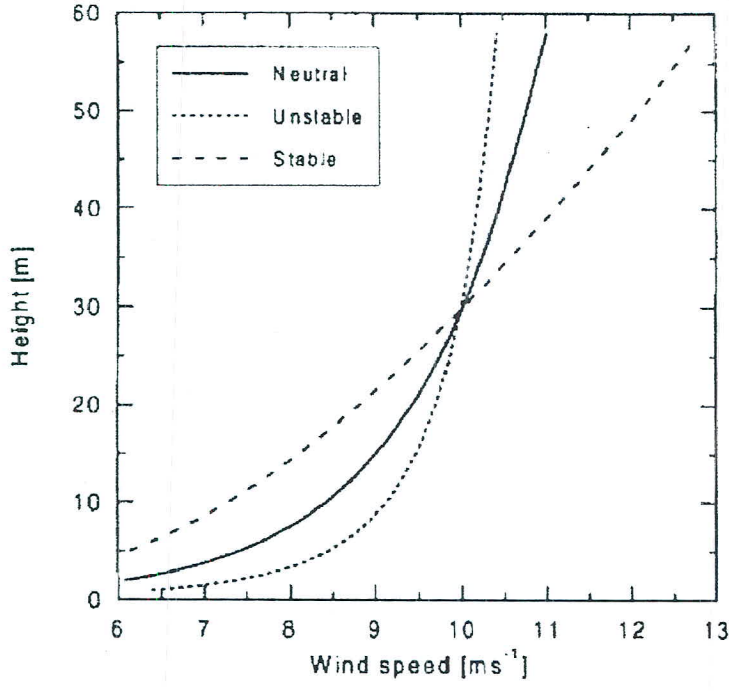

Figure 2.3: Wind speed profiles for neutral, unstable, and stable boundary layer conditions (Source: Petersen et al., 1998)

2.4 Time-series modeling

Time-series analysis is useful for determining the properties of observed data that can be applied to data generation or simulation, and to forecasting. To forecast hourly wind speed, various techniques are available, ranging from simple models to numerical weather prediction (NWP). Table 2.1 shows the various techniques and applications of wind speed and power forecasting. Persistence models are the simplest and typically serve as a comparison to other techniques. NWP uses an atmospheric model to compute key atmospheric states spatially in three dimensions and temporally, and it is generally considered most sophisticated because it requires relatively large computational resources and substantial inputs (e.g. meteorological data for initial and boundary conditions, surface terrain, and land cover) in implementation (Costa et al., 2008; Hill et al., 2012; Lei et al., 2009; Monteiro et al., 2009). Time-series modeling is a forecasting technique whose basic concept is to parameterize selected time-dependent algebraic or polynomial equation using historical data and then predict future values using the fitted formula.

Milligan et al. (2003) proposed the use of statistical wind power forecasting models as an important tool for efficient electrical system operation with wind power plants. Autoregressive moving average (ARMA) models based on historical data from wind farms were used to forecast wind power for a time horizon of 6 hours. The persistence model, which assumes that the value of the future wind speed within the forecast horizon is the same as that observed for the current hour was also used in the study. Different ARMA models had varying performance depending on the forecast horizon, and the potential use of ensemble forecasts would be needed in such situations. Torres et al. (2005) used a similar approach on observed hourly average wind speed data. However, the handling of the historical wind data was different. The data was grouped in monthly subsets to deal with seasonal patterns and then processed to be made stationary. The ARMA models used in the study showed better performance than did the persistence model. Duran et al. (2007) applied autoregressive (AR) models to predict wind power and autoregressive models with exogenous variable (ARX) for forecasting wind speed for look-ahead times of 6, 12 and 24 hours. The performance of the models was assessed against the persistence model and it was seen that the AR and ARX models presented better forecasts than the persistent model for the time horizons considered.

For a case of sites in the South Coast of Oaxaca, Mexico (Cadenas and Rivera, 2007), the autoregressive integrated moving average (ARIMA) and Artificial Neural Network (ANN) models were applied for prediction of wind speed. The study used a 7 year period of observed wind speed data. The models were trained using 6 years of data and then tested within the last year of the dataset. Upon evaluation, the seasonal ARIMA (SARIMA) model was shown to have better performance. Monteiro et al. (2009) suggested the need for wind speed forecasting as a vital technique to address the wind power variability and introduce efficiency into electrical grids with input from wind farms.

Kavasseri and Seetharaman (2009) applied fractional-ARIMA models on observed wind speed from sites in North Dakota (US) with a training period of four weeks. The forecasted values were then applied to a manufacturer's wind turbine curve for wind energy prediction. For three sites in Mexico, Cadenas and Rivera (2010) used ARIMA models for an initial step of wind speed prediction, followed by construction of an ANN from the resulting errors in order to reduce the overall forecasting error of this hybrid model approach. Wind speed predictions were done individually for the cases of the hybrid, ARIMA and ANN models and the performance evaluated for comparative purposes using statistical evaluation criteria. It was found that the hybrid model had better accuracy in all the cases explored for the different sites.

Ewing et al. (2007) under the framework of multivariate analysis, used vector autoregressive (VAR) models to investigate the relationship between wind speeds recorded at different heights (13, 33, 70, and 160 ft) of a meteorological tower in Texas, U.S. The results indicated that the records at 13 ft were the most co-dependent and while those at 70 ft had more autocorrelation. For a case of sites in North Dakota, USA, Erdem and Shi (2011) implemented the short-term forecasting of wind speed and direction through ARMA and VAR models. The VAR models were found to be more favorable for wind direction forecasts rather than for wind speed prediction when compared to the univariate models. An application of VAR models for the generation of multivariate time series of wave and wind condition for marine purposes in the Gulf of Cádiz, Spain, was done by Solari and van Gelder (2011). The artificial series from the VAR models were

able to match the auto-correlation and cross-correlation composition of the original time series.

Hill et al. (2012) applied univariate ARMA and spatial correlation VAR models on wind speed data for 14 sites in the United Kingdom. The adequacy of the models was evaluated from residual diagnostics and forecast performance. The VAR model was found to be suitable for the generation of artificial wind speed data that are representative of the sites. It was shown that the VAR model had upto 19% improvement on persistence for forecasts over 6 hours ahead. It is seen here that ARIMA models tend to represent a major class of well-established fundamental time-series models. There are extensions or variants to ARIMA, one of which is SARIMA. VAR models are an extension of AR class for multivariate data. ARIMA and SARIMA are considered here because they have been widely applied in many disciplines (e.g. finance, energy, and environmental quality), whereas VAR models are continuing to generate interest in these fields as well.

Table 2.1: Wind speed and power forecasting methods (Source: Monteiro et al., 2009)

Forecast category	Approach	Model*	Application
Physical methods	Numerical weather prediction (NWP)	▪ HIRLAM ▪ MM5 ▪ RAMS ▪ WRF	▪ Large-scale area ▪ Long-term prediction ▪ Use of terrain, obstacle, pressure, humidity and roughness as input
Statistical methods	Time series models	▪ Persistence model ▪ ARMA ▪ ARIMA ▪ ARX ▪ Linear regression ▪ Kalman filter	▪ Short-term prediction ▪ Persistence model used as benchmark in very short-term forecasts ▪ Use of historical data from wind farm or monitoring station
Spatial correlation method	–	▪ Spatial correlation	▪ Short-term prediction ▪ Use of spatial relationship and historical data of adjacent sites
Artificial intelligence and new methods	Hybrid structures	▪ ANN + Fuzzy logic ▪ Spatial correlation + NN	▪ Improved forecast accuracy ▪ Use of historical or online data

*Remark
ANN: Artificial Neural Network
ARIMA: Autoregressive, integrated moving average
ARMA: Autoregressive moving average
ARX: Autoregressive with exogenous variable
HIRLAM: High Resolution Limited Area Model
MM5: Fifth-generation Penn State/NCAR Mesoscale Model
NN: Neural Network
RAMS: Regional Atmospheric Modeling System
WRF: Weather Research and Forecasting Model